

Fatigue Considerations of Wavestar Testbench Load Measurements

**Simon Ambühl
Anders Hedegaard Hansen
Enrique Vidal Sánchez
Mikael Pedersen
Morten Kramer**



Aalborg University
Department of Civil Engineering
Reliability, Dynamics and Marine Engineering

DCE Technical Report No. 190

Fatigue Considerations of Wavestar Testbench Load Measurements

by

Simon Ambühl
Anders Hedegaard Hansen
Enrique Vidal Sánchez
Mikael Pedersen
Morten Kramer

June 2015

© Aalborg University

Scientific Publications at the Department of Civil Engineering

Technical Reports are published for timely dissemination of research results and scientific work carried out at the Department of Civil Engineering (DCE) at Aalborg University. This medium allows publication of more detailed explanations and results than typically allowed in scientific journals.

Technical Memoranda are produced to enable the preliminary dissemination of scientific work by the personnel of the DCE where such release is deemed to be appropriate. Documents of this kind may be incomplete or temporary versions of papers—or part of continuing work. This should be kept in mind when references are given to publications of this kind.

Contract Reports are produced to report scientific work carried out under contract. Publications of this kind contain confidential matter and are reserved for the sponsors and the DCE. Therefore, Contract Reports are generally not available for public circulation.

Lecture Notes contain material produced by the lecturers at the DCE for educational purposes. This may be scientific notes, lecture books, example problems or manuals for laboratory work, or computer programs developed at the DCE.

Theses are monographs or collections of papers published to report the scientific work carried out at the DCE to obtain a degree as either PhD or Doctor of Technology. The thesis is publicly available after the defence of the degree.

Latest News is published to enable rapid communication of information about scientific work carried out at the DCE. This includes the status of research projects, developments in the laboratories, information about collaborative work and recent research results.

Published 2015 by
Aalborg University
Department of Civil Engineering
Sofiendalsvej 11,
DK-9200 Aalborg SV, Denmark

Printed in Aalborg at Aalborg University

ISSN 1901-726X
DCE Technical Report No. 190

Recent publications in the DCE Technical Report Series

Fatigue Considerations of Wavestar Testbench Load Measurements

1. Introduction

Wave energy converters (WECs) enable to harvest energy from waves and transfer it to electricity. There exist many different working principles how energy from waves can be harvested. These different working principles lead to diversified WEC concepts. So far none of the concepts reached commercial stage though some concepts exist on prototype level and are moving towards commercialization.

The main focus of the WEC community in general is on increasing the efficiency in order to gain as much as electricity as possible from a given sea state. The efficiency can be increased by optimizing the control system. But the control system does not only drive the efficiency, it also impacts the loads onto the structure, which drive the investment as well as operation and maintenance costs. The overall target for a WEC design and concept is to minimize the cost of energy (COE) in order to become competitive with other renewable electricity sources. Figure 1 shows a sketch indicating the different areas to be considered in order to minimize the COE.

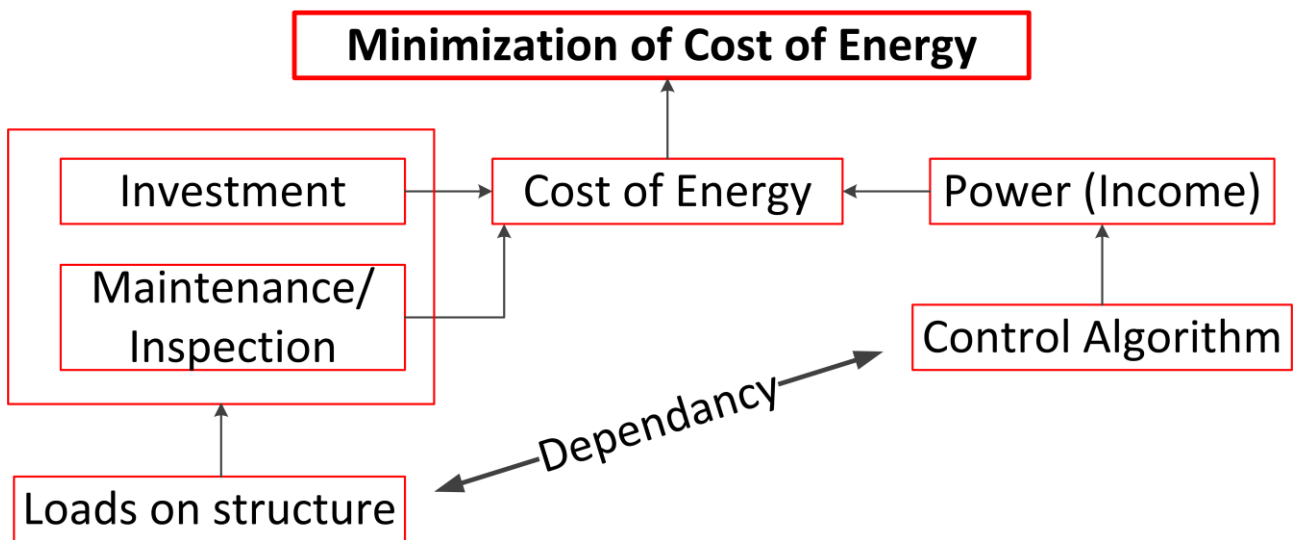


Figure 1: Different areas to be considered when targeting on minimizing cost of energy of a WEC.

One needs to keep in mind that there are also aspects, which are not considered in the simplified sketch in Figure 1 but need to be taken into account like political decisions, environmental restrictions or preferences by the society how their electricity should be produced. Reference [1] shows based on a very simplified approach how different control algorithms impact the COE. This study shows that in order to optimize the device (minimization of COE) it is important to take the load characteristics into account.

One of the most advanced and developed WEC concept is the Wavestar device which is a point absorber device that mainly consists of floaters and a PTO system. The floaters transfer the wave elevation motion into an oscillation mechanical motion which can be used by the PTO system in order to produce electricity. A PTO system is used to transfer the captured wave motion into electricity. The PTO system of the Wavestar device consists of a cylinder which captures the oscillating motion of the floater and transfers it by the use of a hydraulic cycle to a turbine which

drives a generator. A new PTO system is developed which is based on discrete displacement fluid power technology. Power performance results of the new PTO system are published in [2]. The new PTO system enables to reach higher conversion efficiencies due to pace pressure conditions for the generators and the turbine. But this system has discrete force control which transfers the desired smooth force behavior into a stepwise force behavior. The different force characteristics may influence the overall loads onto the structure of the floater and the PTO.

There exist two different loads which are of importance when designing WEC structures. On the one hand the structure is exposed to extreme loads and on the other hand the cyclic loading due to passing waves may lead over time to failure of the structure. This phenomenon is called fatigue. Figure 2 shows some structural components of the Wavestar device which are either more exposed to extreme loads or fatigue loads.

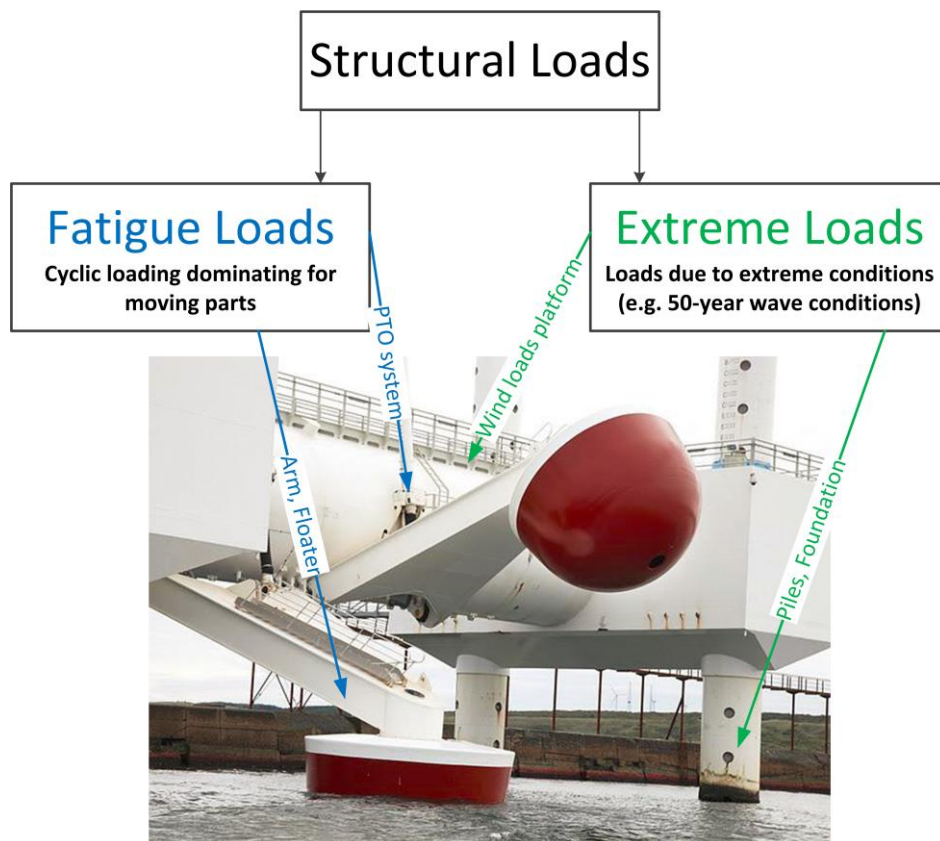


Figure 2: Examples of Wavestar’s structural components, which are either more exposed to fatigue or extreme loads.

At a WEC there exist many moving parts exposed due to its motion to cyclic loading as well as cyclic loading on fixed structural elements due to passing waves. Therefore, fatigue considerations are of importance for WEC structures. Furthermore, it has been shown in other publications (see e.g. [1]) that the control system strongly influences and drives the loads onto the structure. Therefore, an investigation about fatigue loads is of importance and should give an indication on the load characteristics.

Extreme loads during extreme wave and wind conditions are of minor importance for many WEC devices due to the fact that many devices (also the Wavestar device) have a so-called storm protection mode which decreases the loads during storm conditions. For storm protection of the Wavestar device the floaters are moved out of the water. But extreme loads onto the structure can occur during operation when e.g. inauspicious alignments of the waves or failure of the electrical/mechanical systems as well the control system are present. Which failure modes of the system are critical is device dependent and a FTA (Failure Tree Analysis)/FMEA (Failure Modes and Effects Analysis) should be performed before estimating extreme loads given a failure of the system.

This report focuses on fatigue tension loads of the new PTO system of the Wavestar WEC. The purpose is not to perform an optimized design but to give indications about fatigue loads and get a feeling about its characteristic as well as estimates of the fatigue influence of the new PTO system. In this report, not the impact of different control algorithms is investigated, but the impact on the structural loads of a new PTO system enabling higher conversion efficiencies.

2. Information about the Setup and the Location of the Force Measurement Devices

The considered testbench is located at the Department of Energy Technology at Aalborg University and was developed in collaboration with Wavestar. This setup enables to simulate wave loads and measure the power performance of the PTO system as well the corresponding loads. The setup represents a real-scale PTO system of a Wavestar floater.

There are two force sensors, which measure the local loads, mounted at the middle section between the PTO cylinder and the wave cylinder. Figure 3 shows where the force sensors are located on the testbench. The two force sensors have a small difference due to the fact that there is some bending of the middle section when loads are applied. An example of recorded force time series for regular sinus waves is given in Figure 4. The measured loads had a certain offset (different for the two force sensors), which is already subtracted in Figure 4. For fatigue considerations, the explicit force value is less important than the actual amplitude of a load cycle, which remains the same when removing the offset value. The resulting load amplitudes are close to each other for the two measured forces. The measured force time series represent the tension loads at the connection between the floater and the floater. Due to the fact that not the overall floater, but only the PTO system is physically implemented, the testbench as well as the real device may have different friction behaviour which may lead to slightly different load amplitudes.

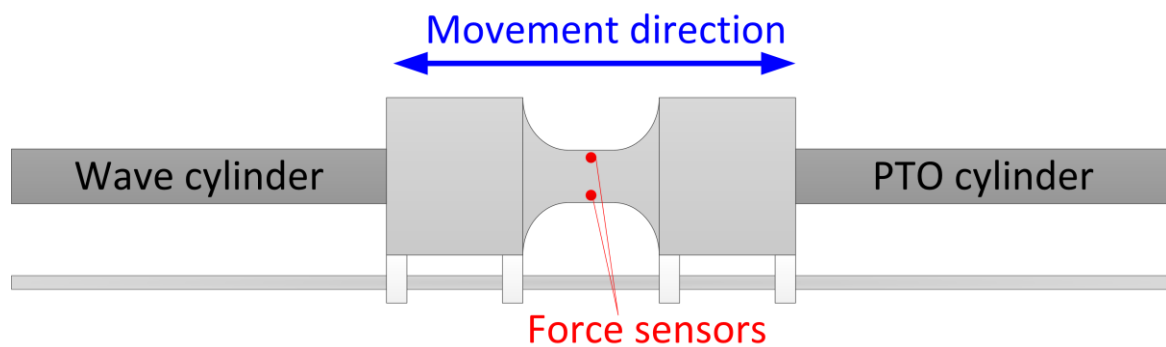


Figure 3: Location of the force sensors on the testbench.

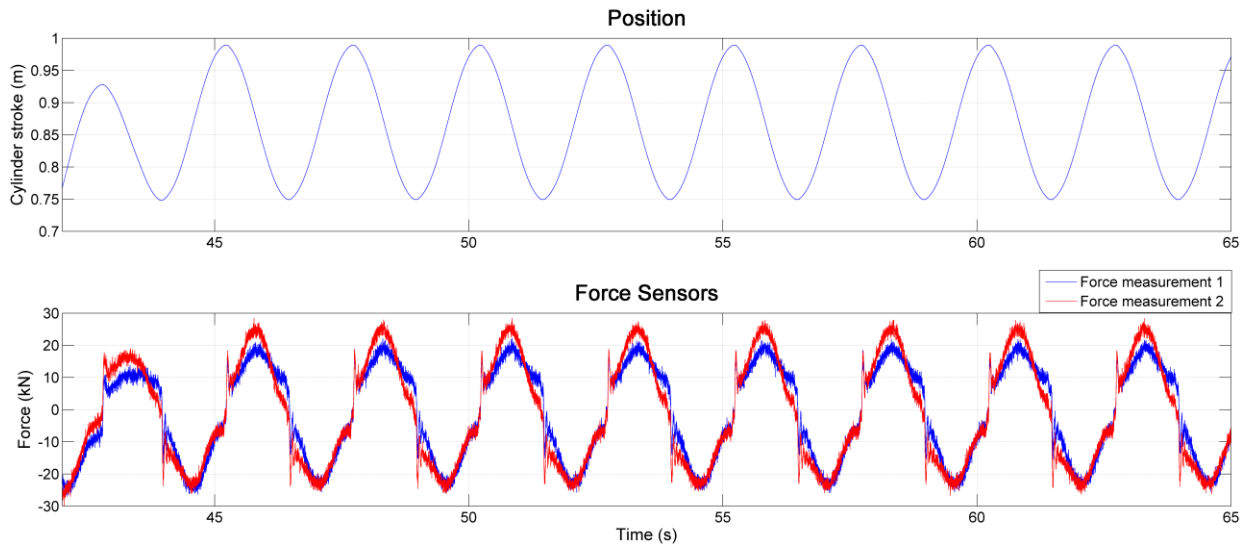


Figure 4: Stroke of the PTO cylinder and the recorded force sensors at the middle section.

3. Considered Environmental Conditions

The environmental conditions considered for this fatigue assessment are taken from sea measurement in the Belgian Sea and shown in Table 1. For significant wave heights larger than 3 meters the floater is lifted out of the water and moved to storm protection mode. At significant wave heights smaller than 0.5 meters the device is not in operation (in storm protection mode) because the power output is too low in order to economically operate the system.

Wind loads during storm protection mode are not considered in this fatigue assessment as well as possible current loads are disregarded here.

Table 1: Scatter diagram with the probability of occurrence of the different wave states.

SS probabilities		T0,2		
		3,5	4,5	5,5
Total	1,000			
Hm0	0,25	not op.	not op.	
	0,75	0,233	0,146	
	1,25	0,083	0,206	
	1,75		0,133	0,071
	2,25		0,038	0,049
	2,75			0,041

There are load time series available for the eleven wave states (9 production modes and 2 with a significant wave height of 0.25 meters) as shown in Table 1. Each load time series contains circa 100 waves. At each time series the first 20 seconds and the last 10 seconds are not considered as there is some transient oscillations at the beginning and some settlement at the end. shows the time series length in seconds for the different wave states. The available total time series length is between 350 seconds and 550 seconds.

Table 2: Available load time series length in seconds for the different considered wave states.

		T0,2		
		3,5	4,5	5,5
Hm0	0,25	350,0	449,9	
	0,75	349,9	450,1	
	1,25	349,7	450,2	
	1,75		450,2	549,8
	2,25		450,1	549,9
	2,75			550,0

4. Background Information about Fatigue

Fatigue covers the failure modes due to cyclic loading. There exist different ways how to treat fatigue. One of the most popular strategy, which is also well established in the industry, is the use of the so-called Miner's rule, SN-curves and rainflow counting. Rainflow counting transfers the load/stress time series into load/stress amplitude distributions. For fatigue assessments not the absolute value of a certain load is most important, but the amplitude of a load cycle. In some cases also the so-called stress ratio R is considered. Some materials (e.g. composites) may have different fatigue characteristics when they are under compression or need to operate under tensile stress conditions. The stress ratio is the ratio between the lowest stress experienced during a load cycle to the highest/maximum experienced stress during the considered stress cycle. The R ratio is important for materials that do not behave in the same way when they are not pre-loaded ($R=0$), under tensile load or tension load. The R -ratio is not considered in the rainflow algorithm used in this report. The rainflow algorithm followed in this study is explained in [3].

The number of cycles leading to failure is dependent on the load amplitude. The relationship between the number of cycles, N_F , of a certain stress range ΔS leading to failure can be expressed by so-called SN-curves. These curves can in their simplest form be described by the Basquin Equation [4], which assumes linear relationship between $\log(\Delta S)$ and $\log(N_F)$:

$$N_F = K \cdot \Delta S^{-m} \quad (1)$$

where K and m are material and structural detail dependent parameters. Plamgren-Miner's rule [5] (also just called Miner's rule) is used to estimate the damage increase per load cycle with a certain amplitude. Miner's rule assumes linear damage accumulation and independence of the cycle occurrence order. The damage increment ΔD_i of one load cycle amplitude equal to ΔF_i is:

$$\Delta D_i = \frac{1}{N_{F,i}} \quad (2)$$

where $N_{F,i}$ is the number of cycles until failure for the load amplitude ΔF_i . The total damage, D_{tot} , after n cycles is equal to:

$$D_{tot} = \sum_{i=1}^n \Delta D_i = \sum_{i=1}^n \frac{1}{N_{F,i}} \quad (3)$$

SN-curves for offshore (steel) applications can be found in [6] and [7]. SN-curves depend among others on the environmental conditions (e.g. humidity or salinity) and the considered corrosion

protection. There are linear and multi-linear SN-curves where the slope m is not constant over the whole stress range. Figure 5 shows an example for different SN-curves. The value m is commonly between 3 and 5. Fatigue failure occurs when the damage D reaches 1.

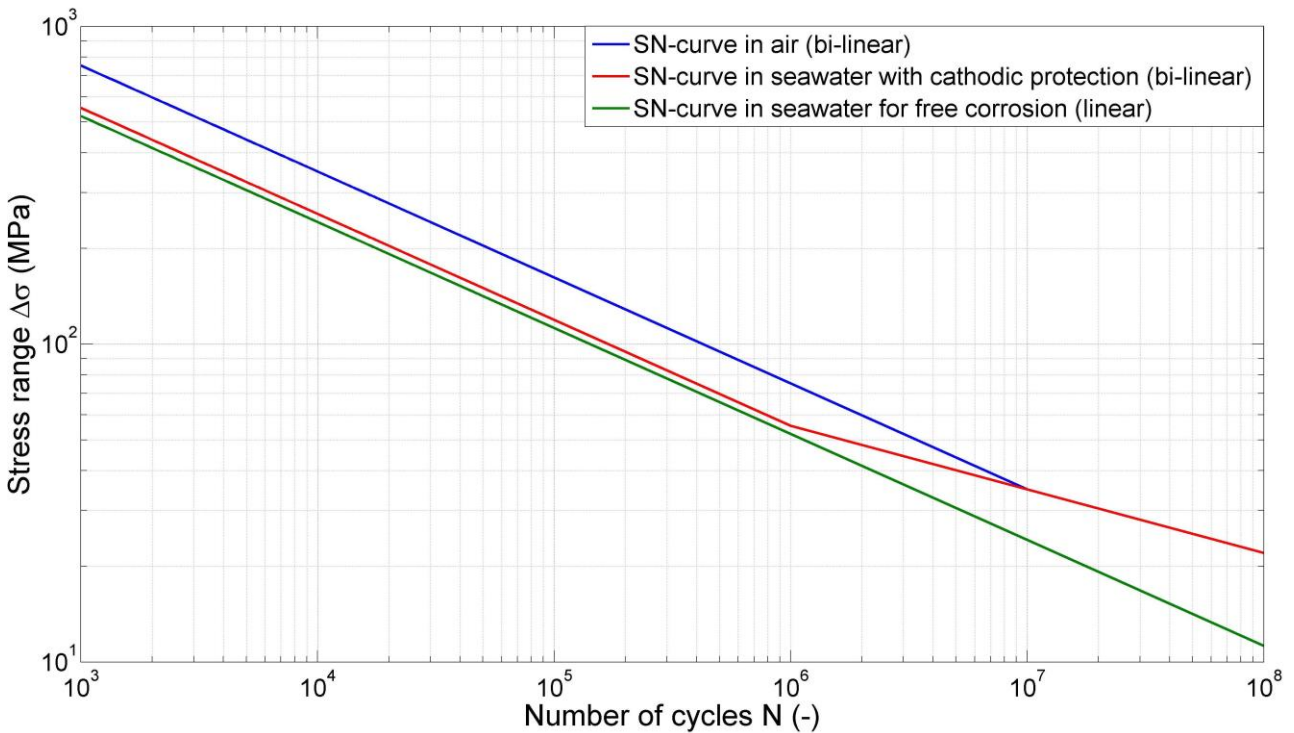


Figure 5: Example of linear and multi-linear SN-curves according to [6] considering a so-called ‘F’-detail.

Another way for fatigue assessments is the use of fracture mechanics. This methodology models the physical background of the fatigue failure: Crack growth. But modelling crack growth is more complex and very detail (including the imperfection leading to crack growth) as well as load characteristic dependent. For research applications the fracture mechanics approach is often used due to the fact that it gives crack development information and enables to investigate the crack evolution directly with modern measurements. But for many industry applications, the fracture mechanics approach is due to its complexity limited applicable.

Not the stresses, which are used for the SN approach, but the loads (normal force at the cylinder) are measured at the testbench. It is not the purpose of this report to verify the structural design of the PTO system, but more to get an idea of the load characteristics in order to make future optimisations. Therefore, among others the so-called equivalent force is considered and compared in this report. The equivalent force shows the force amplitude which leads to the same damage over the lifetime of the component as the considered load spectra from rainflow counting. In order to calculate the equivalent force, the number of cycles remains the same. The equivalent force ΔF_{eq} can be calculated as:

$$\Delta F_{eq} = \left(\frac{1}{N} \sum_{i=1}^N \Delta F_i^m \right)^{1/m} \quad (4)$$

Where N is the number of load cycles to be considered in the load time-series, ΔF_i the corresponding force amplitude of the load cycle i . The larger the equivalent force ΔF_{eq} is, the larger the larger the stresses of a given design and therefore the lower the expected life-time.

5. Results

The load time series presented in Table 3 are available and investigated in this report. What is investigated when comparing the four different load time series with each other is given in Table 4.

Table 3 Explanation of the available load time series.

Denomination	Description
Force 1	Load measured from load transducer at the connection between the two cylinders (including friction loads of the testbench).
Force 2	Load measured from load transducer at the connection between the two cylinders (including friction loads of the testbench).
Continuous reference	Continuous load reference signal from the waves without any safety implementations.
Discrete reference	Discretized continuous reference signal including absolute load limitations at circa 420 kN (safety implementation)

Table 4 The different factors which are investigated when comparing the different load signals.

Compared loads		What does the difference represent?
Force 1	Force 2	Load distribution within the structural detail connecting the two cylinders.
Force1/2	Continuous signal	Impact from friction of testbench as well as influence of absolute load limitations and impact of the discretized PTO system.
Force 1/2	Discrete signal	Impact from friction (from testbench) and difference between measured/modelled discretized PTO systems.
Discrete signal	Continuous signal	Impact of load limitations and the new PTO system (on modelling level).

There are two load measurements available as well as the load signal the piston is aiming for (continuous signal) and the reference step load (discrete signal). The continuous signal does not contain any step functions (including many small oscillations) and will therefore have a smaller number of load cycles compared with the loads time series ‘Force 1’ and ‘Force 2’. The discrete load signal shows the reference signal for the loads ‘Force 1’ and ‘Force 2’.

Table 5 and Table 6 show the equivalent force amplitude (see Equation (4)) for two different m values ($m=3$ and $m=5$). It can be seen that larger significant wave heights or longer wave periods lead to larger equivalent load amplitudes. Furthermore, the equivalent load amplitude is very sensitive to the factor m . A value of $m=5$ leads to at least two times larger equivalent value compared with the results from $m=3$. The differences between ‘Force 1’ and ‘Force 2’ are equal to or smaller than 6.8% for $m=3$ and 5.7% for $m=5$, respectively. The equivalent force amplitude difference between ‘Force 1’ and ‘Force 2’ becomes smaller when increasing H_{m0} or $T_{0,2}$. The equivalent force amplitude of the desired load is smaller for small H_{m0} or $T_{0,2}$ than the equivalent load amplitudes from ‘Force 1’ and ‘Force 2’. The reason for this behaviour lies in the large friction when simulating small wave states with low velocity of the cylinders. Low velocities of the PTO cylinder lead to large friction values. Figure 6 shows a load times series detail for a wave state with small stroke movements. When moving to large H_{m0} values, the PTO system reaches saturation (around 420kN) which is a load limitation. The continuous desired load signal does not include this limitation. An example of a load time series for a large H_S value is given in Figure 7. The measured loads ‘Force 1’ and ‘Force 2’ show are load limited at about ± 420 kN (in Figure 7 the threshold is around +400kN and -440kN due to the fact that the load offset of roughly 20 kN is not considered). Large significant wave heights increase the load measured between the two cylinders. Furthermore, when having large and fast stroke movements, the impact of the testbench friction becomes less important.

Table 5 Equivalent force amplitude for the three recorded (2 Load measurements and the desired load) for $m=3$.

Force 1		T0,2			Force 2		T0,2			Reference continuous load		T0,2		
		3,5	4,5	5,5			3,5	4,5	5,5			3,5	4,5	5,5
Hm0	0,25	6.15	8.02		Hm0	0,25	6.57	8.51		Hm0	0,25	3.44	6.00	
	0,75	10.93	16.80			0,75	11.26	17.24			0,75	9.46	16.35	
	1,25	17.33	21.97			1,25	17.63	22.31			1,25	16.52	22.97	
	1,75		27.45	27.94		1,75		27.69	28.05		1,75		35.18	40.62
	2,25		29.41	30.85		2,25		29.60	30.89		2,25		40.55	57.52
	2,75			31.99		2,75			31.95		2,75			61.51

Table 6 Equivalent force amplitude for the three recorded (2 Load measurements and the desired load) for $m=5$.

Force 1		T0,2			Force 2		T0,2			Reference continuous load		T0,2		
		3,5	4,5	5,5			3,5	4,5	5,5			3,5	4,5	5,5
Hm0	0,25	15.62	22.73		Hm0	0,25	16.50	23.60		Hm0	0,25	9.94	17.39	
	0,75	31.86	50.06			0,75	32.35	50.80			0,75	26.00	46.59	
	1,25	51.43	64.49			1,25	51.75	64.92			1,25	44.30	63.43	
	1,75		77.77	79.16		1,75		78.04	79.21		1,75		93.81	107.89
	2,25		81.89	85.60		2,25		82.16	85.45		2,25		100.29	148.66
	2,75			88.09		2,75			87.83		2,75			149.73

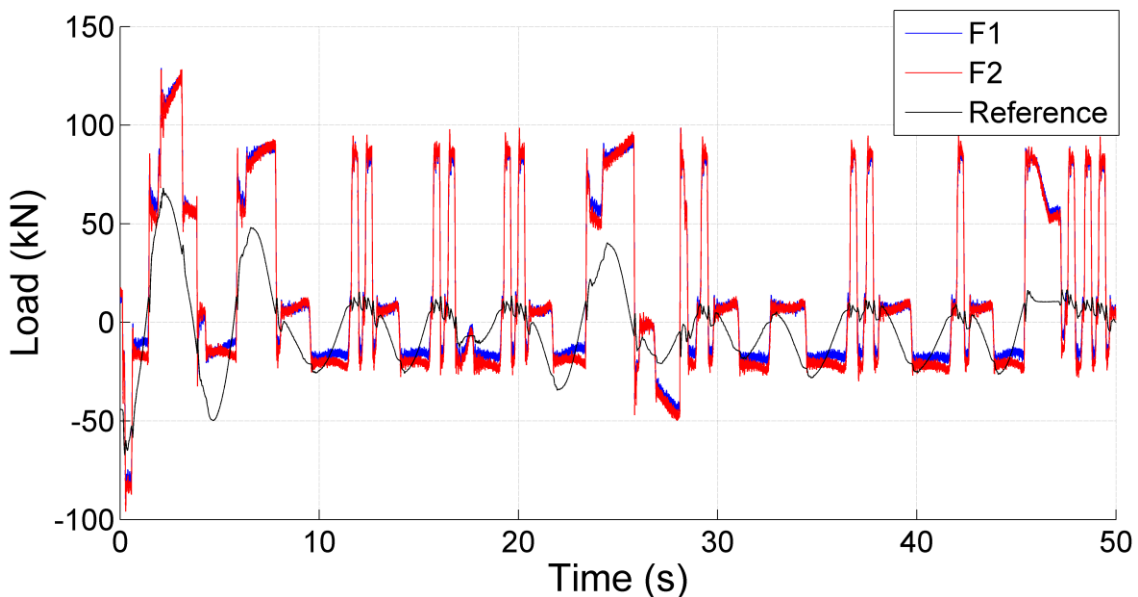


Figure 6 Load time series of the continuous reference load (desired load) and the two measured loads for a wave state with $H_s=0.25$ m and $T_{0,2}=3.5$ s.

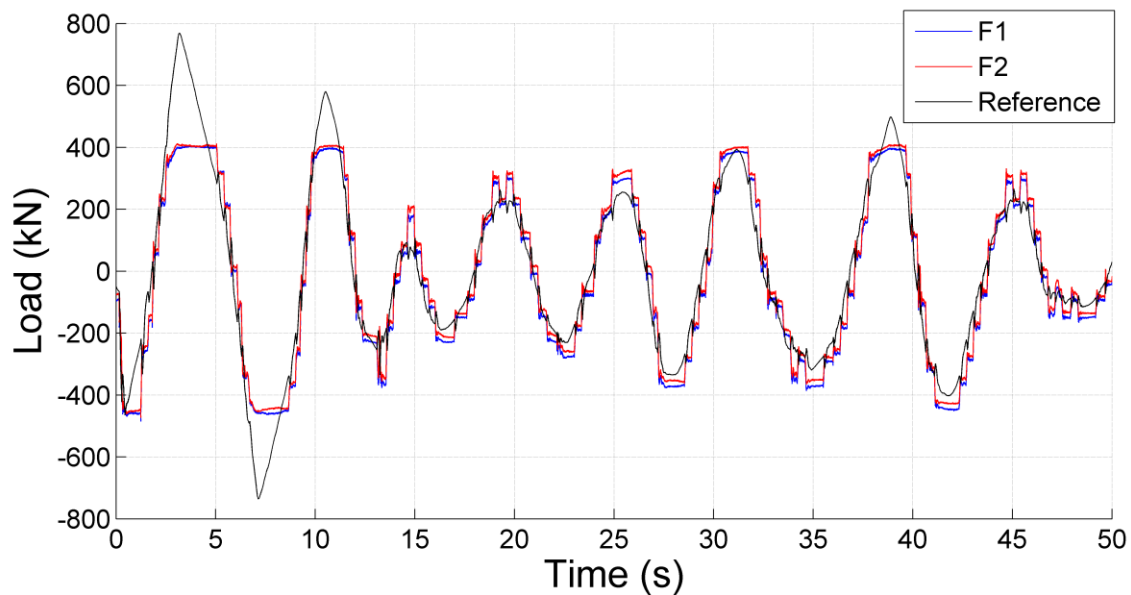


Figure 7 Load time series of the continuous reference load (desired load) and the two measured loads for a wave state with $H_S=2.25$ m and $T_{0,2}=5.5$ s.

When considering fatigue not only the equivalent force but also the number of cycles are of importance. In a next step the equivalent force and number of cycles to be expected during a life time of 20 years are considered. The different wave states and their probabilities of occurrence as shown in Table 1 are considered. Current as well as wind loads (may be of importance during storms when the floaters are moved out of the water) are not taken into account.

The expected equivalent load for $m=3$ and $m=5$ for the three loads (the two different measured loads and the reference load) as well the number of cycles to be expected during a life time of 20 years are shown in Table 7. It can be seen that the equivalent reference force is larger than the equivalent load resulting from the measured forces ('Force 1' and 'Force 2'). The difference among the equivalent load of the two measured loads is 1.1% for $m=3$ and 0.5% for $m=5$. Load 'Force 1' has a larger number of cycles but a smaller equivalent loads compared with load 'Force 2'. This leads to most probably to roughly the same damage over time. The difference of the number of cycles to be expected during 20 years of life time differs by roughly 3% among the two measured load time series. The continuous reference load has roughly 25% larger equivalent loads due to no load limitation (safety measure) but only half the number of cycles as expected when using discrete displacement fluid power technology which leads to a larger amount of small load cycles.

Table 7 Equivalent loads and number of cycles using the wave states shown in Table 1 for an expected life time of 20 years.

	Force 1	Force 2	Reference Force (continuous)
Equivalent load ($m=3$) (kN)	22.54	22.79	28.21
Equivalent load ($m=5$) (kN)	68.00	68.28	87.89
No. of cycles (-)	1.55E+11	1.50E+11	7.21E+10

Largest load cycle amplitudes are in the range of 450 kN (when using an absolute load limitation of circa 420 kN) of the measured load signals 'Force 1' and 'Force 2'. For the reference load the maximum load amplitude is roughly 800 kN (no load limitations).

In order to get an idea about the load characteristics, so-called load spectra are used in order to interpret the load characteristics. Load spectra contain the number of load cycles during a certain amount of time (often the expected life time is taken as reference time) with a certain load amplitude range. In order to accurately present the load characteristics, the overall amplitude range

is divided into 50-100 bins. Figure 8 shows the load spectra for the three considered loads. It can be seen that the most load cycles have small load amplitudes. Circa 99% of all load cycles have amplitudes smaller than 8 kN. Important for fatigue considerations are the large loads, which do not occur often, but have a large impact on the damage. A more detailed picture on the large loads is given in Figure 9 where the range of the y-axis is reduced compared with Figure 8 in order to increase the resolution of the large loads. The number of cycles of the continuous reference load is more or less decaying when moving to larger loads whereas the measured loads show larger fluctuations and the number of cycles does not steadily decrease when the load amplitudes are increased. Reasons for this unsteady behaviour are the discrete displacement fluid power technology leading to step functions as well as the safety mechanism (maximum load of 420 kN) abruptly limits the absolute load value (and also the load amplitudes).

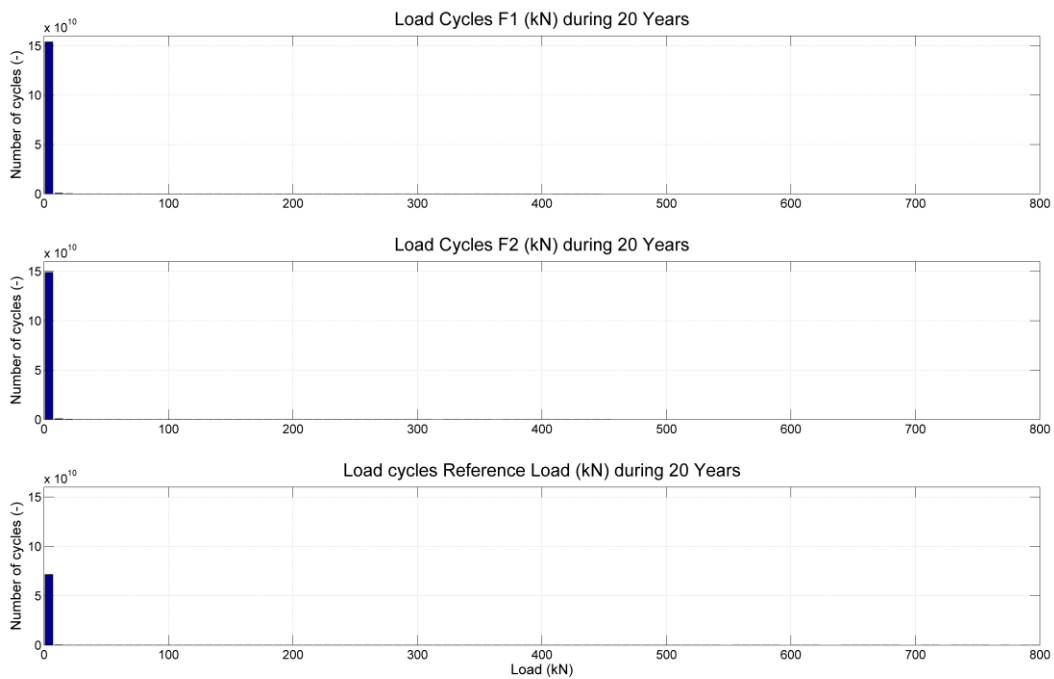


Figure 8 Load spectra for the three loads assuming a life time of 20 years. F1: Measurements from ‘Force 1’; F2: Measurements from ‘Force 2’; Reference load: continuous load reference (no load limitation).

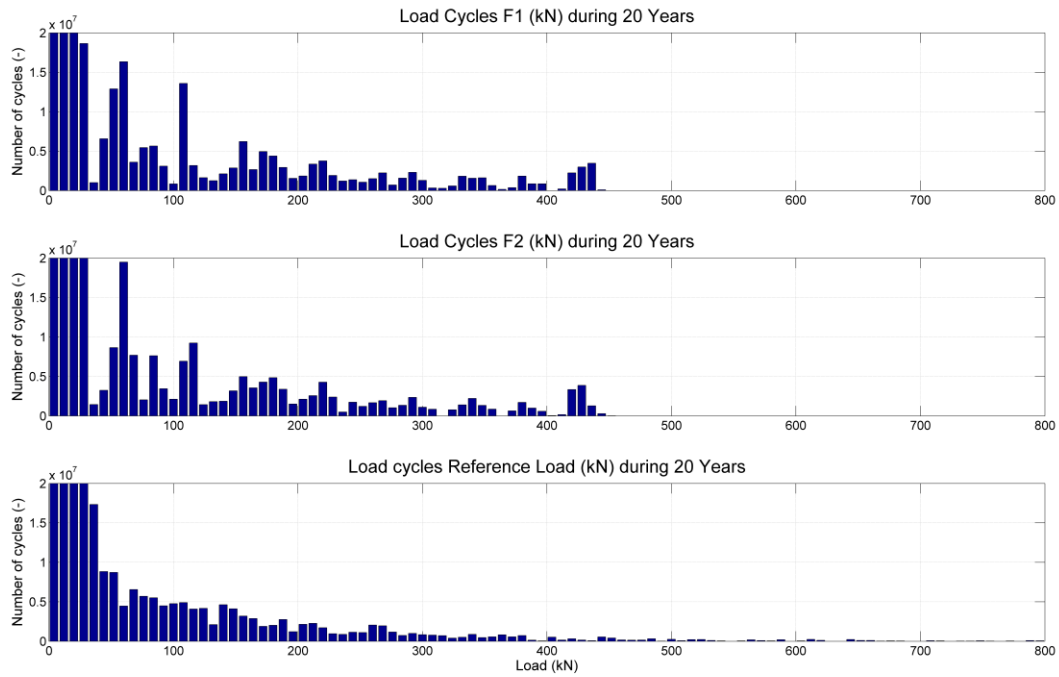


Figure 9 Load spectra (load cycles within life time of 20 years) of the three load time series available with focus on the large loads. F1: Measurements from ‘Force 1’; F2: Measurements from ‘Force 2’; Reference load: continuous load reference (no load limitation).

The results in Table 7 are based on no post-processed load time series data. Commonly measured data contains noise which is also considered in the results presented in Table 7. Noise consideration is the reason for high number of cycles (in the range of 10^{11} within a life time of 20 years) which is in the range of 200 load cycles per second. This number of cycles per second is quite high. In order to become a realistic estimation of number of load cycles per second, one needs to get rid of the noise signals. When considering measured data often the first bin of the load spectra (see Figure 8) is not considered assuming that the load cycles due to noise have small amplitudes. This procedure makes sure that noise, which consists of many small fluctuations of the load, is not taken into account. In this case when removing the bin with the lowest load cycle amplitudes only load cycles with amplitudes larger than 8 kN are considered. This procedure impacts the equivalent load values as well as the number of load cycles to be considered during a life time of 20 years. The results are shown in Table 8. The equivalent load is increased compared with the case presented Table 7 and the number of load cycles is lowered. Furthermore, the expected load cycles to be expected during a life time of 20 years are in the range of 10^9 , which leads to roughly 1.5 load cycles per second.

Table 8 Equivalent loads and number of cycles larger than 8 kN using the wave states shown in Table 1 for an expected life time of 20 years.

	Force 1	Force 2	Reference Force (continuous)
Equivalent load (m=3) (kN)	114.30	111.87	142.33
Equivalent load (m=5) (kN)	180.34	177.45	232.23
No. of cycles (-)	1.18E+9	1.26E+9	5.59E+8

From the before mentioned characteristics, it is difficult to directly estimate what the differences mean in practice with respect to costs and different designs (dimensions). Therefore, in order to estimate the impact of the displacement fluid power technology onto the structure, a simple fatigue analysis is performed.

The (minimal) rod size (diameter) of the PTO cylinder is designed here with focus on fatigue loading. Figure 10 shows the location of the considered detail as well as the corresponding load direction. It is assumed that the cylinder is exposed to axial loading, which leads according to [6] to the so-called bilinear SN-curve of a ‘B1-detail - operating in air’. The considered SN-curve parameters are given in Table 9. A bilinear SN-curve is used which means that the slope of the curve is changed (here at $N=10^7$ cycles).

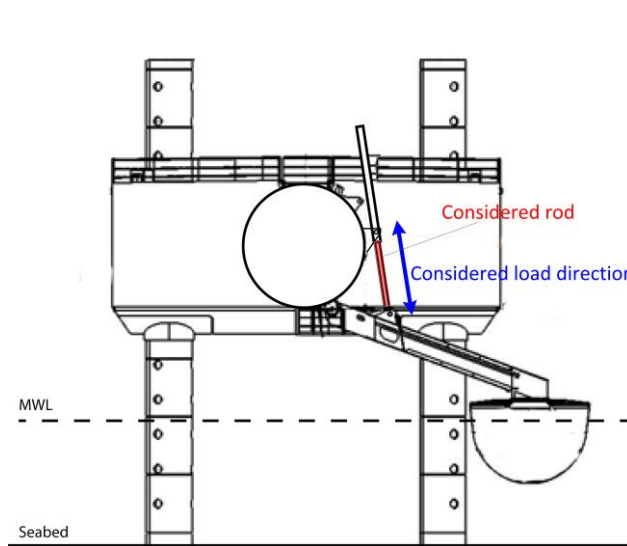


Figure 10: Location of considered detail (rod of PTO cylinder) and the corresponding load direction.

Table 9 Bilinear SN-curve of detail 'B1' operated in air.

$\log(K_1)$	m_1	$\log(K_2)$	m_2
15.117	4.0	17.146	5.0

Structural designs based on SN-curves consider stress amplitude values and not directly load amplitudes. Therefore, the loads need to be transferred into stresses. Due to the fact that axial loading is assumed, the stress amplitude $\Delta\sigma$ can be estimated easily from a certain load amplitude ΔF by:

$$\Delta\sigma = \frac{\Delta F}{z} \quad (5)$$

where z is the corresponding cross section area. The cross section area is the parameter to be designed in this example.

When performing structural designs, safety factors, which account for uncertainties not considered in deterministic designs, need to be considered. For structural designs with focus on fatigue so-called Fatigue Design Factors ($FDFs$) are considered. This value is based on the time as fatigue is a time-dependent process.

The FDF value is larger than or equal to 1 and defines the ratio between the amount of years considered for the design (T_{FAT}) in years as well as the expected life time in years (T_L):

$$FDF = \frac{T_{FAT}}{T_L} \quad (6)$$

Appropriate FDF values are defined in standards. Due to the fact that no standards for WEC applications exist so far, guidelines for offshore wind turbines can be followed due to the fact that offshore wind turbines as well as WECs have the same (low) consequences in case of failure and

are therefore designed with the same reliability level. According to [8] for structural details of offshore wind turbines are *FDF* values chosen equal to 3. This number is also considered here. The design of the rod may also be dependent on other failure modes like e.g. buckling as well as the dimensions/standard designs of different rods available on the market.

It needs to be kept in mind that using the same *FDF* value for different load characteristics means that the probability of failure will be different. When calibrating safety factors, probabilistic reliability assessments should be performed in order to calibrate *FDF* values with respect to a certain reliability level. The question whether or not a *FDF* value of 3 is appropriate for this detail is not answered in this report.

Table 10 shows the results of the rod design using different loads. When taking the discrete reference signal, the resulting rod diameter is 10% less compared with the measured loads ‘Force 1’ and ‘Force 2’. This means that the small fluctuations and the friction of the testbench increase the rod diameter by roughly 10%. It is expected that the difference between the discrete reference signal and the measured loads ‘Force 1’ and ‘Force 2’ is mainly driven by the friction due to the fact that friction has a large impact for small wave states (see e.g. Figure 6) and the small waves have larger probabilities of occurrences than the larger wave states.

A 15% larger rod diameter results when taking the continuous load signal instead of the discretized load signal. This means discretization and limitation of the load enables to decrease the rod diameter by roughly 15%.

The diameter of the rod varies less than 0.2% when considering either the load signal ‘Force 1’ or ‘Force 2’. This difference is small compared with the friction impact or the load influence due to absolute load limitations.

In this design so far, noise signals are considered due to the fact that the measured data is considered. The rod dimensions are shown in Table 11 when disregarding noise signals by only considering load cycles with an amplitude larger than 8 kN. The rod design values from considering the noise signals (Table 10) as well as disregarding the noise signals (Table 11) are negligible – differences are in the range of 10^{-5}mm^2 . This means the considered fatigue modelling approach (rainflow counting) is not sensitive to noise signals.

Table 10 Results of the rod dimensions using different load time series.

	Force 1	Force 2	Reference continuous force	Reference discrete force
Resulting cross sectional area (mm³)	5455.90	5439.48	5992.10	4518.63
Rod diameter (mm)	83.35	83.22	87.35	75.85

Table 11 Results of the rod dimensions considering only load amplitudes larger than 8 kN (preventing taking noise into account) using different load time series.

	Force 1	Force 2	Reference continuous force	Reference discrete force
Resulting cross sectional area (mm³)	5455.90	5439.48	5992.10	4518.63
Rod diameter (mm)	83.35	83.22	87.35	75.85

6. Conclusions

The new PTO system leads to more load cycles (increase by a factor of 2) compared with a continuous load signal. But 99% of all cycles measured at the two force transducers are smaller than 8 kN and have therefore small impact on the fatigue.

Important in order to decrease the fatigue is the limitation of the absolute load onto the floater by using safety valves. The absolute load limitation of 420 kN decreases the large load cycles from 800 kN (no load limitations) down to 430 kN. A simple fatigue-based design of the rod size of the PTO cylinder shows that the force limitation enables to decrease the rod diameter by roughly 15%.

A difficulty for the analysis of the available data is the friction of the testbench which is of importance when considering wave states with small (and slow) stroke movements. It is not possible to quantify the friction based on the available data and therefore separate the load impact of the load fluctuations due to pressure fluctuations inside the pressure pipes and the friction impact. Consideration of the testbench friction and pressure load fluctuations make a 10% larger rod diameter necessary compared with the modelled discretized load signal. It is expected that the friction impact (leading to larger load amplitudes) on the fatigue design is much larger than the many small load cycles due to pressure fluctuations within the pressure pipes.

Investigations on the design with and without noise signal treatments showed that the considered fatigue procedure is not sensitive on noise interactions due to the fact that the noise cycle amplitudes are small and their impact on the fatigue design is negligible even though the number of small load cycles is large.

7. References

- [1] Ferri, F.; Ambühl, S.; Fischer, B.; Kofoed, J.P. Balancing Power Output and Structural Fatigue of Wave Energy Converters by Means of Control Strategies. *Energies* **2014**, *7*, 2246-2273.
- [2] Hansen, R.H.; Kramer, M.M.; Vidal, E. Discrete Displacement Hydraulic Power Take-Off System for the Wavestar Wave Energy Converter. *Energies* **2013**, *6*, 4001-4044.
- [3] ASTM Standard for Cycle Counting Fatigue Analysis; ASTM Standard E 1049-85; American Society for Testing and Materials (ASTM): New York, NY, USA, 2005.
- [4] O. H. Basquin. The exponential law of endurance tests. *American Society for Testing and Materials (ASTM)*, 10(2):625–630, 1910.
- [5] M. A. Miner. Cumulative damage in fatigue. *Journal of Applied Mechanics*, 12(3):159–164, 1945.
- [6] DNV-RP-C203. Fatigue Design of Offshore Steel Structures. Technical report, Det Norske Veritas, 2010.
- [7] ISO 19902:2007. Petroleum and Natural Gas Industries – Fixed Steel Offshore Structures. Technical report, International Organization for Standardization (ISO), 2007.
- [8] DNV-OS-J101. Design of offshore wind turbine structures. Technical report, Det Norske Veritas, 2013.

